CONSERVATION
SCIENCE PARTNERS

TECHNICAL REPORT
30 September 2022

For the project entitled:

The role of U.S. agricultural lands in supporting avian species connectivity

Submitted to:

American Farmland Trust

Recommended citation: Conservation Science Partners (CSP). 2022. The role of U.S. agricultural lands in supporting avian species connectivity. Final Report. Truckee, CA.

Noteʏ wefeɪ·ăe oƭ odzℕ ăɪ·∃e ∃ℕodzăe ϒɪ·LJă ɭă LJeyŘɭy∃℗ ¢o eyãdzℕe odzℕ ϒɪ·LJLJɭy∃ ɭă dzăɭy∃ tKe ϒoăt Ŏdzℕℕeyƭ ɭyƭoℕϒɪ·tɬoyΣ ǿe LJfɪ·y′to ℕeØɭeǿ ɪ· ℕeÔeyƭfè ℕefeɪ·ăeŘ ℕeLJoℕt oy′ɪ· ϒ′dzfttɭπèeɪ·ℕ ăɪ·∃e ∃ℕodzăe LJℕo?eÔt ōè ɪ· Ôoyfão℡tɭdzϒ oƭ ƬeŘeℕɪ·f ɪ·∃eyÔɭeă℗

CALIFORNIA HEADQUARTERS
11050 PIONEER TRAIL • SUITE 202
TRUCKEE, CALIFORNIA • 96161
(P) 530.214.8905 • (F) 530.214.8907

INFO@CSP-INC.ORG
WWW.CSP-INC.ORG

Background

Agricultural lands (cropland, pasture, and rangeland) account for almost half of the land area of the conterminous United States (CONUS) and are frequently implicated in species declines through habitat loss and fragmentation, pesticide use, and the impacts of mowing and harvest (Newbold et al. 2015, Stanton et al. 2018). However, the effects of agriculture on wildlife populations vary considerably depending on agricultural management practices and the ecology and life history of the species concerned. For some species, agriculture lands may provide important foraging or breeding habitat (Fajardo et al. 2009, Fehlmann et al. 2021) or serve as movement corridors through more heavily modified landscape (Doherty and Driscoll 2018, Grass et al. 2019), while for other, more sensitive species, agriculture may impose hard barriers to movement (Sieving et al. 1996, Wimberly et al. 2018), potentially driving population declines through habitat fragmentation. This range of agricultural impacts is exemplified by avian species, which vary substantially in their capacity to use agricultural landscapes as primary or movement habitat. Agricultural intensification across North America has been a major driver of declines in farmland-associated bird species since the middle of the last century (Stanton et al. 2018). However several authors have noted the potential for supporting avian biodiversity on agricultural lands through wildlife-friendly farming practices and the promotion of functional connectivity across agricultural and mixed-use landscapes (Fahrig et al. 2011, Redlich et al. 2018, Hendershot et al. 2020). Identifying opportunities to support bird species habitat use and connectivity on agricultural lands is therefore an important conservation objective.

Here, we examine the effects of agriculture on habitat suitability and functional connectivity for three avian focal species that exemplify the complex effects of agriculture on species habitat use, movements, and populations: the greater sage grouse (*Centrocercus urophasianus*; hereafter, sage grouse), the American black duck (*Anas rubripes*; hereafter, black duck), and the bobolink (*Dolichonyx oryzivorus*). The sage grouse is experiencing ongoing range contractions, due in part to conversion of their required sagebrush-steppe habitat to agricultural uses, including intensive grazing (Shirk et al. 2017). Despite these grazing impacts, rangelands across the sage grouse's extant range are thought to provide important movement habitat and are typically less strongly avoided than cultivated croplands (Tack et al. 2019). The black duck, once the most common waterfowl species in eastern North America, has experienced substantial declines since at least

the 1950's (English et al. 2017). Conversion of wetland habitat to agricultural and urban uses has been a major driver of declines for this wetland-dependent species (Conroy et al. 2002). However, in recent years, evidence is emerging that agricultural lands may actually provide important wintering and/or nesting habitat for black duck populations, with anthropogenic food subsidies in agricultural fields potentially partially compensating for the loss of preferred wetland foraging habitat (Maisonneuve et al. 2006, Lieske et al. 2012, English et al. 2017). The bobolink is a neotropical migrant songbird that historically nested in native grasslands in the northern US and southern Canada (Herkert 1997). Bobolinks have also experienced substantial population declines (>70% decline since 1968; Stanton et al. 2018) linked to agricultural intensification. With the loss of native grasslands in North America, the majority of bobolink breeding now occurs in pastures and grain fields (Herkert 1997), and major ongoing threats to bobolink populations are linked to the intensity of agricultural management in these systems, i.e., the frequency and intensity of cutting, harvesting, and grazing in agricultural fields (Perlut et al. 2008).

These three focal species differ substantially in their movement capacity and thus their use of agricultural and other modified landscapes. The sage grouse is the least vagile of the three species, consisting of a mixture of resident and relatively short distance (up to ~120 km) migrant populations (Tack et al. 2012, 2019). The relatively limited movement of sage grouse, combined with range contraction, has resulted in restricted gene flow between populations (Oyler-Mccance et al. 2005) and genetic isolation of remnant populations in Washington (Shirk et al. 2017), highlighting the importance of maintaining and restoring connectivity across the sage grouse range. The black duck exhibits intermediate movement capacity, with most populations undertaking seasonal migrations between the southeastern U.S. and the northeastern U.S. and Canada, with multiple stopovers (up to 5) during the course of the migration (Coluccy et al. 2020, Peck et al. 2022). The most vagile focal species is the bobolink, a neotropical migrant that transits between breeding grounds in the northern U.S. and southern Canada and wintering grounds in central South America, a migration that includes trans-oceanic non-stop flights of up to 3,500 km (Perlut 2018).

Given these substantial differences in movement capacity and resulting differences in each species' response to landscape structure and human disturbance, we examined different aspects of landscape connectivity for each of the three focal species. For the sage grouse, we examined connectivity across the sage grouse range during all seasons to capture movements associated with migration as well as natal and breeding dispersal. For the black duck, we examined connectivity between potential stopover sites during spring and fall migration, focusing our analyses on movements occurring between migration start and end dates. Because bobolinks are capable of undertaking non-stop flights of distances greater than the north-south extent of the conterminous United States (Perlut 2018), localized human disturbance and land cover are likely to be less relevant to migratory movements for this species than for the other focal species. However, movement within a breeding season - either natal dispersal outside a parents' territory or dispersal by breeding adults after a failed nesting attempt - has the potential to impact metapopulation persistence and species range contraction/expansion (Fajardo et al. 2009, Cava et al. 2016). Bobolinks show high breeding site fidelity when returning from wintering grounds, but adults and especially fledglings may make exploratory movements within a breeding season to assess potential new breedings sites for the subsequent year. We focused here on these within-breeding season exploratory movements, which are likely to be affected by local/regional landscape characteristics and are therefore a valuable target for connectivity modeling.

For all focal species, we conducted U.S. range-wide analyses of both habitat suitability and connectivity, using random forest models to associate species detection/non-detection data to a suite of habitat covariates (including agricultural land management intensity) and modeling connectivity using circuit theory models. We then discuss the implications of our focal species habitat management in agricultural landscapes.

Methods

Focal species data

For each of the three focal species (sage grouse, black duck, and bobolink), we modeled habitat suitability using detection data from eBird, the Cornell Lab of Ornithology's community science platform (Sullivan et al. 2014, Johnston et al. 2021). eBird data are organized into "checklists", semi-structured surveys in which the observer records the species observed as well as variables

associated with observation effort. Datasets made available for use in research are subject to a rigorous pre-screening procedure (e.g., to remove false positives) and can be filtered to only include "complete" checklists, i.e., those in which the observer recorded all species detected. By using only complete checklists, eBird data provide information on both detections and non-detections of focal species, where non-detections are simply checklists in which the focal species was not observed (Johnston et al. 2021). Community science data are known to be subject to several challenges, including spatial bias (e.g., observers tend to collect data near cities and roads) and substantial variation in sampling effort (e.g., number of observers, duration of surveys, distance traveled). To circumvent these issues, we followed the best practices for using eBird data in scientific research described by Johnston et al. (2021) and Strimas-Mackey et al. (2020), conducting spatial subsampling to remove spatial bias, filtering data by observation effort to reduce variation in effort between checklists, and including effort covariates in our habitat suitability models to account for differences in detection probability between checklists (see below).

We used data from the November 2021 release of the eBird Basic Dataset (EBD), available at www.ebird.org/science/download-ebird-data-products. Following Strimas-Mackey et al. (2020), we filtered the EBD to only include complete checklists and reduced variation in sampling effort by only retaining checklists with ≤ ten observers, duration ≤ 5 hrs, and total travel distance ≤ 5 km. We then created focal species datasets from the filtered EBD by retaining all checklists (both detections and non-detections) within each species' geographic range. We used range maps from the International Union for the Conservation of Nature (IUCN) for each of the three focal species (BirdLife International and Handbook of the Birds of the World 2016a, 2016b, 2021), clipped to the borders of the conterminous United States. Finally, we truncated each species-level data set to only include data collected between 2014 and 2018 in an effort to align detection data with the year of our agricultural and other human land use intensity covariates (2016, see below). As noted above, for the sage grouse, we modeled habitat suitability and connectivity across all seasons, and therefore retained all checklists between 2014 and 2018. Our black duck models focused on connectivity between stopover sites during annual migration. We therefore truncated our black duck dataset to include only detections/non-detections occuring between the minimum start data and maximum end date for both spring and fall migration (spring migration: April 18 to

June 28; fall migration: October 5 to December 18; (Coluccy et al. 2020)). To examine within-breeding season connectivity for bobolink, we truncated our bobolink dataset to only those checklists occurring between the beginning and end of the breeding season (May 1 to September 14; Perlut et al. 2008, Perlut 2018).

For each focal species, we performed spatiotemporal subsampling on detection and non-detection data. As discussed in detail by Strimas-Mackey et al. (2020), spatiotemporal subsampling is effective in dealing with several common modeling issues affecting community science data, including spatial and temporal bias (e.g., tendencies for community members to conduct sampling close to home and/or only in favorable seasons; Luck et al. 2004, Courter et al. 2013, Sullivan et al. 2014) and class imbalance, i.e., substantial differences in the number of datapoints coded as detections vs. non-detections (Robinson et al. 2018). Detection data, particularly for rare species, is often highly imbalanced, with far more non-detections than detections (REF). Of the three focal species, sage grouse had the most limited geographic range, as well as the smallest total number of checklists and the lowest proportion of detections relative to non-detections (0.3% of 321,034 checklists). Given the relatively limited amount of available information on where sage grouse are present, we followed guidance in Robinson et al. (2018), retaining all checklists in which sage grouse were detected and spatially subsampling non-detection checklists by randomly selecting a single non-detection checklist within each cell of a 10 x 10 km grid overlaid across the sage grouse's geographic range. This resulted in a total of 1,277 detection and 2,782 non-detection checklists (nominal 31.5% detection rate).

Both black duck and bobolink have much larger geographic ranges and a substantially larger number of eBird checklists. We therefore performed spatiotemporal subsampling of all checklists for each species, randomly selecting one detection and one non-detection checklist for each year of the study (2014 to 2018) within each cell of a 20 x 20 km grid overlaid across each species' geographic range (note the larger grid cell size relative to sage grouse to accommodate the much larger geographic ranges of black duck and bobolink). This resulted in 7,140 detection and 38,514 non-detection checklists for black duck (18.5% detection rate) and 11,335 detection and 46,663 non-detection checklists for bobolink (24.3% detection rate). We prepared eBird datasets using the *auk* package (Strimas-Mackey et al. 2018) in R (R Core Team 2021).

Model covariates

For each focal species, we modeled habitat suitability as a function of several environmental and climatic covariates, described in detail below (see also Table 1). Following the best practices for research with eBird data, we quantified all covariates within a 2.5 km radius of each checklist location, corresponding to the spatial precision of the species detection data (maximum travel distance for checklists included here = 5 km) and representing an ecologically relevant scale for many bird species (Strimas-Mackey et al. 2020, Johnston et al. 2021). Covariate values for each checklist location were calculated as either the mean value or percent cover within the specified radius and were derived by first calculating the focal mean (for continuous covariates) or focal sum (for binary covariates) at each pixel using circular kernels with a 2.5 km radius and then extracting these smoothed values for the pixel associated with each checklist location. To facilitate prediction from habitat suitability models, we also extracted smoothed values of all relevant covariates at all pixels within a 250 m x 250 m grid spanning each species' geographic range, buffered by the relevant movement distance for each species (see Connectivity modeling section below for more on relevant movement distances).

For all species, we quantified mean human land use intensity, *L*, using the *L* layers described in detail in Appendix A (see also CSP 2019) and based on a procedure originally developed by Theobald (2013). These *L* layers integrate multiple datasets to estimate the intensity of disturbance at each location (i.e., raster pixel) across the landscape for four categories of human disturbance: agriculture, urbanization, transportation, and energy development. *L* values for each disturbance type range between 0 and 1 and are based on underlying datasets quantifying human land use circa 2016. For all non-agricultural disturbance types we utilized existing *L* layers (CSP 2019). For agricultural land use intensity, we developed a novel *L* layer that incorporates high-resolution data on agricultural land uses from the American Farmland Trust's Farms Under Threat analysis (CSP 2020) and remotely sensed estimates of management intensity at all cropland and pasture pixels (Appendix A). For the present analysis, we extracted values from each of the four *L* layers at each eBird checklist location, allowing us to consider, e.g., the effect of agricultural land use intensity on species habitat suitability separately from that of other disturbance types. We also included topographic covariates in all models, including mean

elevation, slope, aspect, and ruggedness (an estimate of the variability in slope and aspect within a given neighborhood). All topographic variables were calculated using the ALOS World 3D Digital Surface Model (30 m resolution; Takaku et al. 2016). Ruggedness was estimated using the vector ruggedness metric (VRM) with a window size of 1 km (Sappington et al. 2007).

For each focal species, we included one or more land cover covariates describing habitat types known to be important to that species. Sage grouse are dependent on sagebrush habitat (Connelly et al. 2000, Tack et al. 2012, Zeller et al. 2021) and we therefore included the percent cover of sagebrush, using the LANDFIRE v2.0 Existing Vegetation Type (EVT) dataset (LANDFIRE 2016) filtered to only those cover types with "sagebrush" in the EVT name. Black ducks are strongly associated with coastal and inland aquatic habitats for both nesting and foraging, including open water (lakes, ponds, rivers), wetlands, and tidal flats (Morton et al. 1989, Maisonneuve et al. 2006, Lieske et al. 2012, English et al. 2017). We used the 2016 National Land Cover Database (NLCD; Dewitz 2019) to quantify the percent cover of open water (NLCD code 11), all wetlands (90, 95), and herbaceous wetlands (95), isolating the latter category because of the potential importance of herbaceous wetlands in providing emergent vegetation on which black ducks can forage (English et al. 2017). We also quantified the percent cover of tidal flats circa 2015-2016 using the dataset developed by Murray et al. (2019). Bobolinks breed in grasslands and agricultural fields (pastures), and tend to avoid other cover types such as forested areas (Herkert 1997, Bollinger and Gavin 2004, Perlut et al. 2008). We used the NLCD to calculate percent cover of forests (NLCD codes 41-43) and shrublands (52). To develop a comprehensive estimate of grassland percent cover, we combined the footprints of the NLCD grassland and pasture/hay classes (71, 81) with that of pastures identified by the Farms Under Threat 2016 land cover layer (CSP 2020).

Finally, we included one or more climate covariates for each focal species, with all climate covariates derived from NASA's Daymet v4 dataset (Thornton et al. 2020). For sage grouse, we included mean daily snow water equivalent during winter months (01 November to 01 April), as snow cover can limit sage grouse access to forage (Homer et al. 1993, Tack et al. 2012). For sage grouse and bobolink, we included the mean daily minimum and maximum temperatures, and for all three species, we included mean daily precipitation. Because the majority of black duck

detections occurred within the northern portion of their range, temperature covariates were largely confounded with latitude in model predictions, leading to predicted suitable habitat that was largely confined to northern areas and thus limiting our ability to analyze connectivity across the black duck's entire U.S. range. We therefore excluded temperature covariates from the black duck model and relied instead on precipitation and land cover/use. We calculated averages for minimum and maximum temperatures and precipitation across the entire year for sage grouse. For black duck and bobolink, we calculated means during the focal periods (i.e., spring/fall migration and breeding season, respectively). We extracted climate variables for the relevant periods between 2014 and 2018, corresponding to the timespans of the eBird detection datasets described above. Table 1 provides a summary of all covariates and the models in which they were used. All covariates were compiled, processed, and exported at 250-m resolution using Google Earth Engine (GEE; Gorelick et al. 2017) and the GEE Python API.

Table 1. Descriptions of the spatial covariates used in random forest habitat suitability models for each focal species

Covariate name	Source	Date	Native Resolution	Predictor type	Sage grouse	Black duck	Bobo-link
Agricultural land use intensity	this study	2016	250 m	focal mean	x	x	x
Urban land use intensity	this study	2016	250 m	focal mean	x	x	x
Transportation land use intensity	this study	2016	250 m	focal mean	x	x	x
Energy land use intensity	this study	2016	250 m	focal mean	x	x	x
Elevation	ALOS Global DSM (AW3D)[1]	2021	30 m	focal mean	x	x	x
Slope	ALOS Global DSM (AW3D)	2021	30 m	focal mean	x	x	x
Aspect	ALOS Global DSM (AW3D)	2021	30 m	focal mean	x	x	x
Ruggedness	ALOS Global DSM (AW3D)	2021	30 m	focal mean	x	x	x
Sage brush	LANDFIRE v2.0: Existing Vegetation Type[2]	2016	30 m	percent cover	x		
Water	NLCD 2016[3]	2016	30 m	percent cover		x	x
Herbaceous wetlands	NLCD 2016	2016	30 m	percent cover		x	
All wetlands	NLCD 2016	2016	30 m	percent cover		x	
Forest	NLCD 2016	2016	30 m	percent cover			x
Shrub	NLCD 2016	2016	30 m	percent cover			x
Grassland	NLCD 2016 & Farms Under Threat[4]	2016	30 m, 10 m	percent cover			x
Tidal flats	Murray et al. 2019	2014-2016	30 m	percent cover		x	
Snow-water equivalent	NASA Daymet V4[5]	2014-2018	1 km	focal mean	x		
Maximum temperature	NASA Daymet V4	2014-2018	1 km	focal mean	x		x
Minimum temperature	NASA Daymet V4	2014-2018	1 km	focal mean	x		x
Precipitation	NASA Daymet V4	2014-2018	1 km	focal mean	x	x	x

[1]Takaku et al. (2016); [2]LANDFIRE (2016); [3]Dewitz et al. (2019); [4]CSP (2020); [5]Thornton et al. (2020)

Random forest models of habitat suitability

We fit random forest (RF) models to detection/non-detection data for each species to predict the probability of encountering the species at a given location as a function of environmental and climatic covariates. RF models present several benefits for ecological classification and prediction problems, including high classification accuracy and the ability to deal with complex interactions and collinearity between covariates (Cutler et al. 2007, Fox et al. 2017).

Our process for fitting RF models to eBird data closely followed that described by Strimas-Mackey et al. (2020). For each species, we classified detection/non-detection data based on the spatial covariates described in Table 1 as well as a suite of covariates accounting for variation in detection probability between checklists (Johnston et al. 2021). These detection probability covariates included checklist year, Julian date, start time, duration, total distance traveled, and number of observers. Given that RF models have been shown to be robust to the inclusion of low-importance covariates (Fox et al. 2017), we fit a single model for each focal species, including all detection probability covariates and the environmental and climatic covariates shown in Table 1. Prior to model fitting, we randomly split each species' dataset into training (80% of checklists) and test sets (20% of checklists), using the training sets to fit RF models and the test sets to assess model accuracy. Using the *ranger* package in R (Wright and Ziegler 2017), we fit RF models to training data for each species using 500 trees and partitioning based on the Gini index (Cutler et al. 2007). To further reduce issues related to class imbalance, we used a balanced random forest approach in which, for each tree, an equal number of bootstrapped samples were selected from detections and non-detections (Strimas-Mackey et al. 2020). We set the RF algorithm to predict probabilities rather than binary classification (Malley et al. 2012), which in this case provides an estimate of the encounter rate for the focal species at each checklist location. To validate our models, we quantified their ability to predict withheld test data using five validation metrics: mean squared error, sensitivity, specificity, area under the receiver-operator characteristic curve (AUC), and the kappa statistic (Hastie et al. 2009). We used partial dependence plots (Cutler et al. 2007), which show the marginal effect of a given covariate averaged across all other covariates, to visualize the relationship between individual covariates and species encounter rates.

We used the validated RF models for each species and continuous rasters of spatial covariates to predict encounter rate across each species' geographic range (buffered by relevant movement distance, see below). We treated these predictions as spatially explicit estimates of habitat suitability, assuming that the probability of encountering a species will be higher in more suitable habitat. Following Strimas-Mackey et al. (2020), we accounted for detection probability in our habitat suitability surfaces by making predictions for a "standard" eBird checklist (travel distance = 1 km, duration = 1 hr, number of observers = 1) in the year 2016 and setting the Julian date and checklist start times to those with the highest detection probability for each species (sage grouse: 18 March at 05:02; black duck: 17 December at 05:05; bobolink: 13 May at 05:05). Habitat suitability surfaces ranged between 0 and 1 and were derived at 250 m resolution.

Connectivity modeling

We ran omnidirectional connectivity models for each focal species using the Omniscape algorithm (McRae et al. 2016, Landau et al. 2021), a circuit theory-based approach that models the movement of organisms across the landscape as the flow of electrical current through a circuit (McRae et al. 2008, Dickson et al. 2019). In circuit theory-based models, current flow provides an estimate of the probability or intensity of the movement of organisms through every pixel on the landscape. Omniscape models "coreless" connectivity in which every pixel may potentially serve as a source and/or target of movement, thus allowing current to potentially flow in all directions. Inputs for Omniscape models include a source strength surface, describing the predicted probability or intensity of movement from a given location, and a landscape resistance surface, which estimates the difficulty an animal experiences in moving through each pixel on the landscape (Zeller et al. 2012). For each focal species, we used the habitat suitability surface to define source strength, thresholding the layer to only those pixels with habitat suitability greater than 0.2 to avoid treating the least suitable pixels as potential sources of animal movement (McRae et al. 2016)**.** Following Keeley et al. (2016), we used a negative exponential function to transform habitat suitability into landscape resistance, *R*, via

$$R = 100 - 99 * ((1 - \exp(-c * h)) / (1 - \exp(-c))),$$

where h is the habitat suitability value at a given pixel and c is a constant that determines the degree of nonlinearity between h and R. Lower values of c produce linear or nearly linear relationships between h and R, while higher values of c produce increasingly non-linear relationships such that resistance declines more quickly with increasing values of habitat suitability. Following guidance in Keeley et al. (2016), we chose a c value resulting in a moderately non-linear relationship between h and R ($c = 8$).

The Omniscape algorithm uses a moving window approach, iteratively treating every pixel in the source strength layer with a value greater than zero as a target for electrical current and connecting that pixel to all other non-zero pixels within the moving window radius, which serve as current sources. The moving window size thus sets the maximum distance between movement start and end points. For each focal species, we determined the moving window size based on the animal's movement capacity and the seasonal/life history period over which analyses were run, referred to elsewhere in the text as the 'relevant movement distance'. Because our sage grouse model addressed all seasons and movements, we treated the maximum observed movement distance in the literature (120 km; Tack et al. 2012, 2019) as the relevant movement distance. This distance also captures recorded maxima for natal and breeding season dispersal (Dunn and Braun 1986, Cross et al. 2017). For the black duck model, which focused on connectivity between migratory stopover sites, we considered the relevant movement distance to be 250 km, comparable to the average distance between stopover sites for all populations monitored by Coluccy et al. (2020). For the bobolink model analyzing within-breeding season dispersal movements, we used the maximum observed distance between breeding sites (or natal site and first breeding site) for a single individual (approx. 10 km; Fajardo et al. 2009) as our relevant movement distance. Fajardo et al. (2009) measured natal/breeding dispersal distances as the distance between sites used in consecutive breeding seasons (i.e., separated by migration to winter range and back). However, we assume here that these distances are a reasonable approximation of the distances bobolinks will travel *within* a breeding season when undertaking exploratory movements to assess potential new breeding sites (Cava et al. 2016). Connectivity models were run in the Omniscape.jl software package in Julia (Landau et al. 2021).

For each species, we compared current flow on agricultural lands with current flow on other land cover/land use types by first sampling a large number of current flow values at random locations distributed across each species' geographic range. The total number of points sampled was proportional to the total area of each species's range, equaling approximately 5 random samples per 100 km^2 (sage grouse: n = 105,608; black duck: n = 213,089; bobolink: n = 236,833). We classified each random point as falling into one or more of the following categories: *cropland*, *pasture*, *rangeland*, *woodland*, or *all agriculture* (i.e., any one of the previous four categories), based on the FUT 2016 land cover layer (CSP 2020); *low density development,* based on the 2016 NLCD (Dewitz 2019) (NLCD classes: 'developed, open space' and 'developed, low intensity' categories); *high density development* (NLCD classes: 'developed, medium intensity' and 'developed, high intensity' categories); *natural land cover* (all NLCD non-agricultural vegetation categories, i.e., cover classes 41-74 and 90-95); and *protected areas* (all public lands in the USGS Protected Areas of the US Database v2.1(USGS 2020) categorized as GAP status 1 or 2, i.e., permanently protected and managed for natural land cover). Agricultural, developed, and natural land categories were mutually exclusive, and we gave preference to FUT agricultural land cover classes where these overlapped with low density development or natural lands. Other categories were non-exclusive; for instance, some natural land pixels were also in protected areas and vice versa. Random point sampling and extraction were conducted in GEE.

Results and discussion

Our validation procedure indicated strong predictive power for each of the three focal species random forest models (Table 2), with all AUC scores > 0.8 and all Cohen's Kappa values > 0.4. (We note that, while there is disagreement in the literature on how to interpret Cohen's Kappa, values above 0.4 are often considered "good" and those above 0.75 "excellent" (Fleiss et al. 2013).) The sage grouse model showed particularly strong capacity to predict out-of-sample data, potentially due to the limited geographic range of this species relative to the other focal species and the strong association between sage grouse and sagebrush-steppe habitat (Tack et al. 2012, Zeller et al. 2021).

Table 2. Validation metrics for each of the focal species random forest models

	Mean squared error	Sensitivity	Specificity	AUC	Kappa
Sage grouse	0.076	0.75	0.967	0.944	0.744
Black duck	0.118	0.637	0.916	0.899	0.528
Bobolink	0.153	0.621	0.852	0.831	0.435

Partial dependence plots, showing the marginal effect of a given covariate averaged across all other covariates in the random forest model (Strimas-Mackey et al. 2020), highlight the complex relationship between agricultural land use intensity (*L*) and habitat suitability for each species (Fig. 1). Encounter rates generally increased with increasing agricultural *L* for sage grouse (Fig. 1a), whose range overlaps substantially with private rangelands but also includes some cultivated areas (Tack et al. 2019). Recent evidence suggests that black ducks may use agricultural lands (croplands and pasture) for foraging during the winter and breeding seasons (Maisonneuve et al. 2006, Lieske et al. 2012, English et al. 2017). However, our model suggests that agricultural lands provide relatively poor stopover habitat during migration, with black duck migratory season encounter rates tending to decline with increasing agricultural *L* (Fig. 1b). Bobolinks exhibited the highest breeding season encounter rates at intermediate values of agricultural *L* (Fig. 1c). As noted above, with the loss of native grasslands, bobolinks now largely depend on grain fields and pastures for nesting (Herkert 1997) but are sensitive to intensive management regimes that involve frequent harvest or mowing (Perlut et al. 2008). The observed peak in bobolink encounter rates at intermediate *L* values likely reflects a preference for pastures and grain fields with less intensive management practices. It should be noted that the patterns in Figure 1 incorporate complex interactions with other environmental and detection-related covariates in the random forest model, which are not straightforward to visualize in partial dependence plots (Strimas-Mackey et al. 2020).

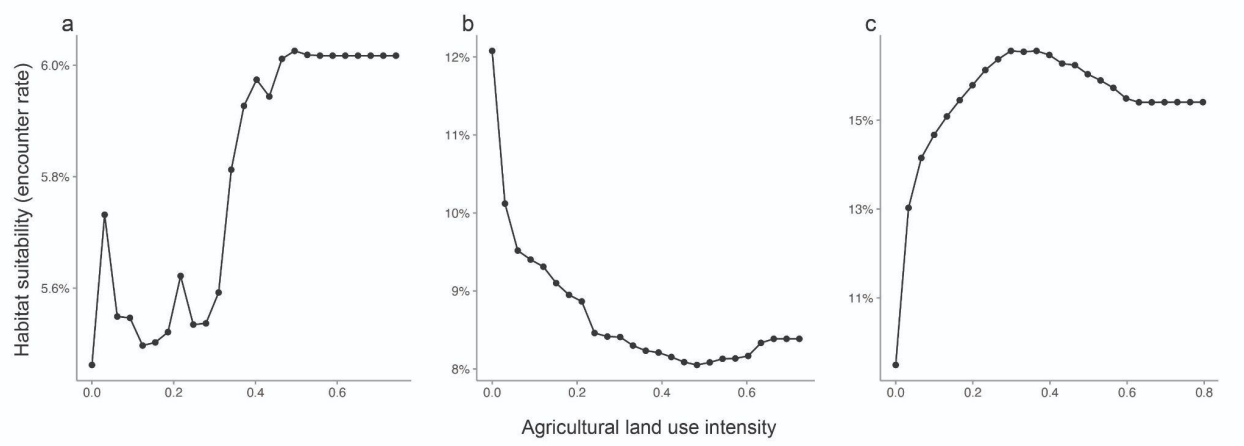

Figure 1. Partial dependence plots of the marginal effect of agricultural land use intensity on encounter rate (a proxy for habitat suitability) for (a) greater sage grouse, (b) American black duck, and (c) bobolink, as estimated by the random forest model for each species.

Maps of habitat suitability and connectivity across each species' geographic range (Fig. 2) highlight potential target areas for management action to preserve high-quality habitat and connectivity within and among populations. Generally, year-round habitat suitability for sage grouse, as well as areas of highest predicted probability of movement (i.e., current flow) were concentrated in relatively flat, medium-to-high elevation (i.e., >1000 m) habitats with high percent cover of sagebrush (Fig. 2a,d). Habitat suitability and connectivity for migrating black ducks was strongly associated with water, being highest in coastal areas, along major river systems, and in the vicinity of the Great Lakes (Fig. 2b,e). Bobolink breeding habitat suitability and connectivity was relatively diffuse throughout the Midwest and Northeast regions of the U.S. (Fig. 2c,f), reflecting this species' use of agricultural landscapes as nesting habitat and general avoidance of forested areas for breeding (Herkert 1997, Bollinger and Gavin 2004, Perlut et al. 2008).

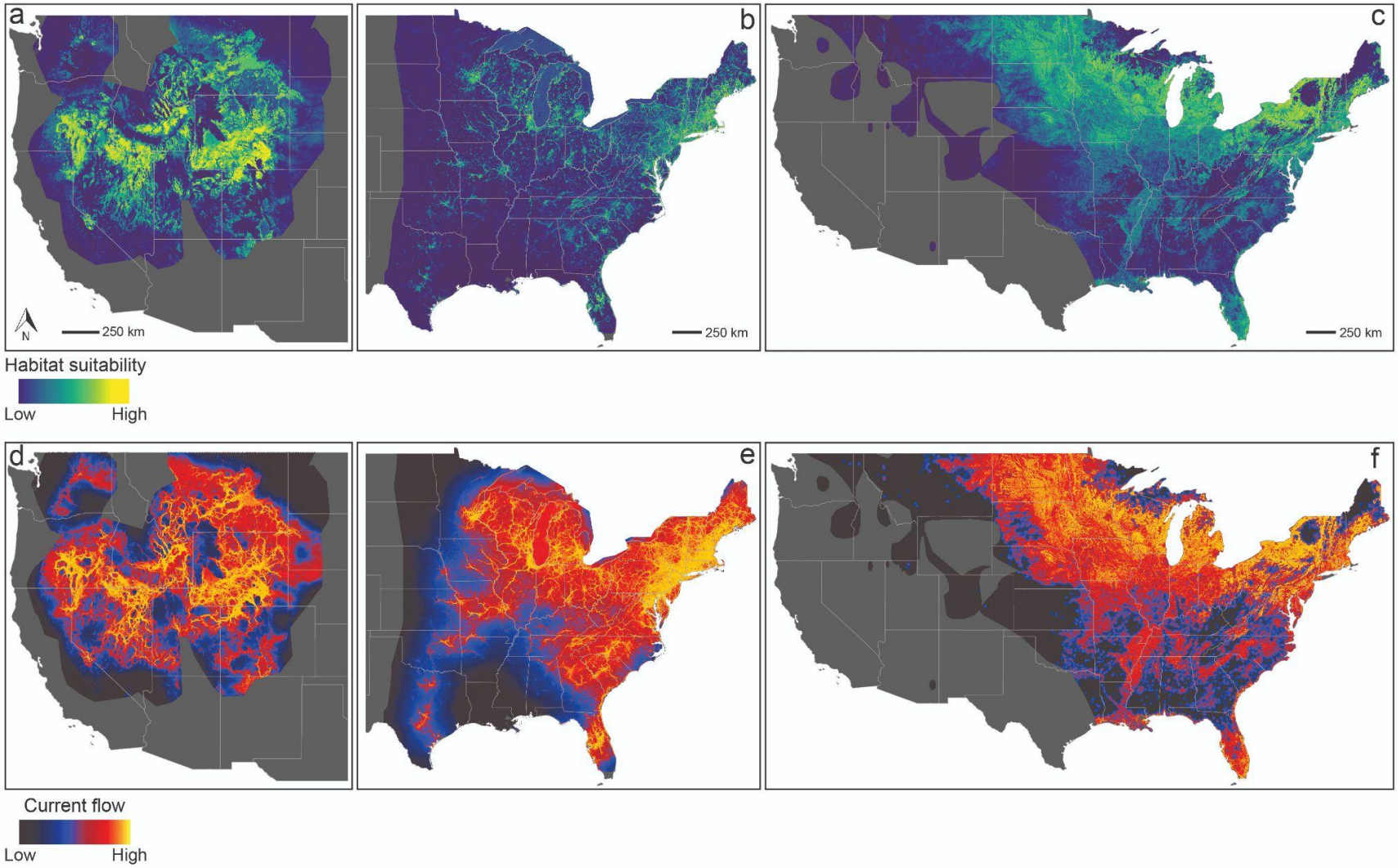

Figure 2. Habitat suitability (as predicted from random forest models) and the predicted probability of movement (i.e., current flow, as predicted from circuit theory-based connectivity models) for greater sage grouse (a,d), American black duck (b,e) and bobolink (c,f).

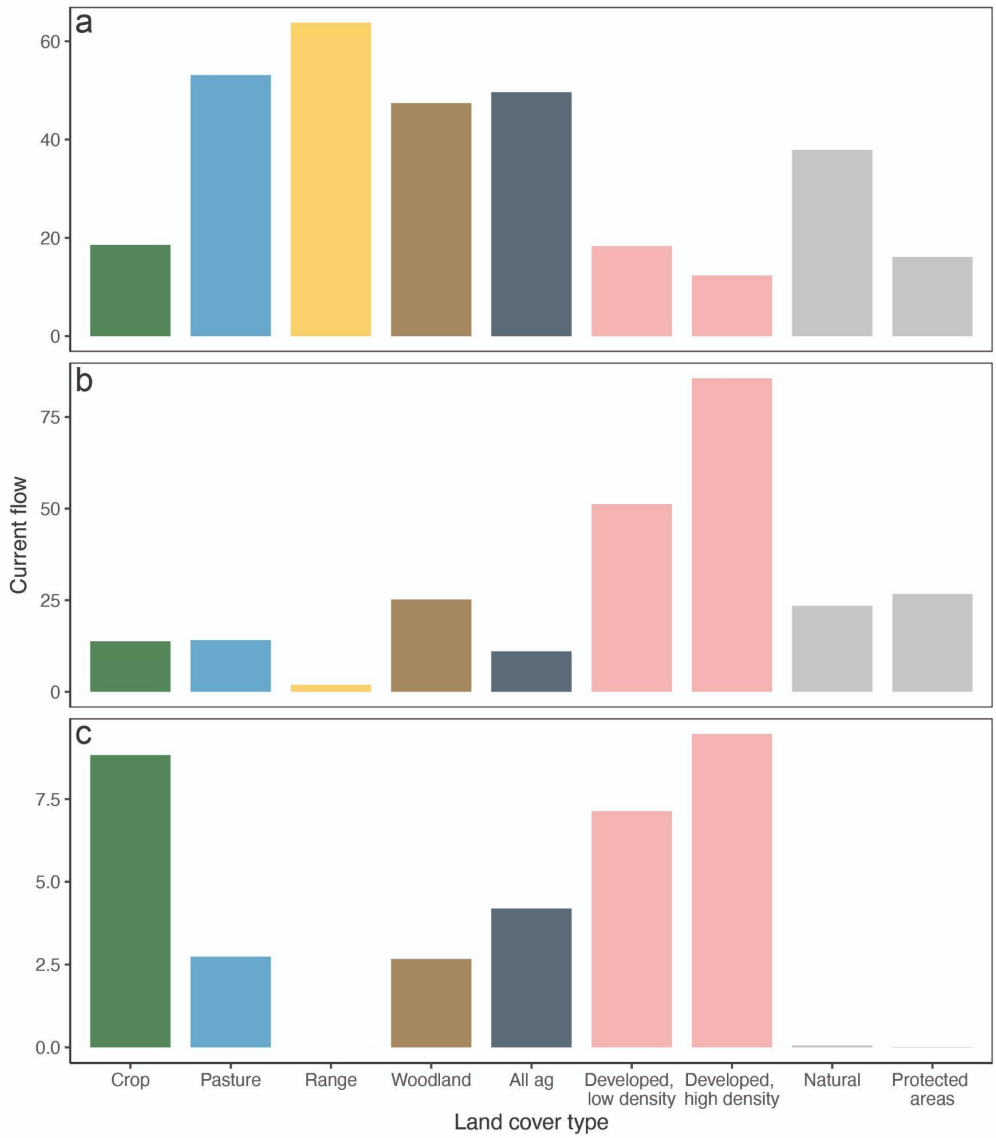

Figure 3. Median current flow values on agricultural lands (cropland, pasture, rangeland, woodland, and all agricultural categories combined ['all ag']) for each focal species, as compared to median current flow in developed areas and landscapes characterized by more natural land cover (i.e., all natural lands and lands within USGS GAP 1 and GAP 2 protected areas). Median current flow values are shown for (a) greater sage grouse, (b) American black duck, and (c) bobolink. Note that, given differences between connectivity model inputs, current flow values are not comparable across species and should only be interpreted here in terms of relative differences between different land cover/land use types

Agricultural lands, and particularly rangelands, provide essential movement habitat for sage grouse, with median current flow values being higher on rangelands than any other land cover/land use type considered (including protected areas and those categorized as having natural

land cover; Fig. 3a). This result confirms previous findings that private lands (particularly ranchlands) in the western U.S. play an important role in supporting sage grouse movement (Tack et al. 2019), providing critical pathways through areas of increased disturbance such as energy development (Doherty et al. 2008). Our model also predicts some sage grouse movement through croplands (Figs. 2d and 3a), and indeed cultivated landscapes have previously been shown to support sage grouse, but only when intermixed with sagebrush steppe habitat (Shirk et al. 2017). Conservation easements that preserve relatively intact rangelands and programs that support the maintenance of native vegetation on cultivated landscapes (e.g., USDA's Conservation Reserve Program) will therefore be critical to sage grouse conservation on working landscapes.

Current flow for migrating black ducks tended to be lowest on agricultural lands relative to more developed or natural land cover/land use types (Fig. 3b), though woodlands (patches of remnant forest cover associated with a functioning farm unit) were predicted to provide some support for black duck movement, as indicated by moderate median current flow values. Generally low predicted movement of black ducks on agricultural lands likely stems from this species' dependence on wetlands, coastal areas, and other aquatic habitats as migratory stopover sites (Stevens et al. 2003, Robinson et al. 2016). Preventing further conversion of aquatic habitats to agriculture or other uses will therefore be critical to ensuring the preservation of high quality stopover habitat for black ducks. While our results suggest limited potential for agricultural lands to support black duck connectivity during migration, previous work indicates a role for croplands and pastures in providing foraging opportunities for ducks during other times of the year (e.g., overwinter; Maisonneuve et al. 2006, Lieske et al. 2012).

For bobolink, croplands exhibited among the highest median current flow values of any land cover/land use type (Fig. 3c), emphasizing the importance of cultivated landscapes for this species during the breeding season (Herkert 1997, Bollinger and Gavin 2004, Perlut et al. 2008). Agricultural lands throughout the eastern and midwestern US will likely continue to play a critical role in supporting breeding season movements of bobolinks (Fig. 2f), particularly where "land sharing" conservation approaches (i.e., practices that maintain or enhance the capacity of farms to support biodiversity through wildlife-friendly farming practices) are encouraged

(Kremen and Merenlender 2018, Grass et al. 2019). The federal government can play a role in supporting such wildlife-friendly practices through programs such as the USDA's Conservation Stewardship Program or Environmental Quality Incentives Program.

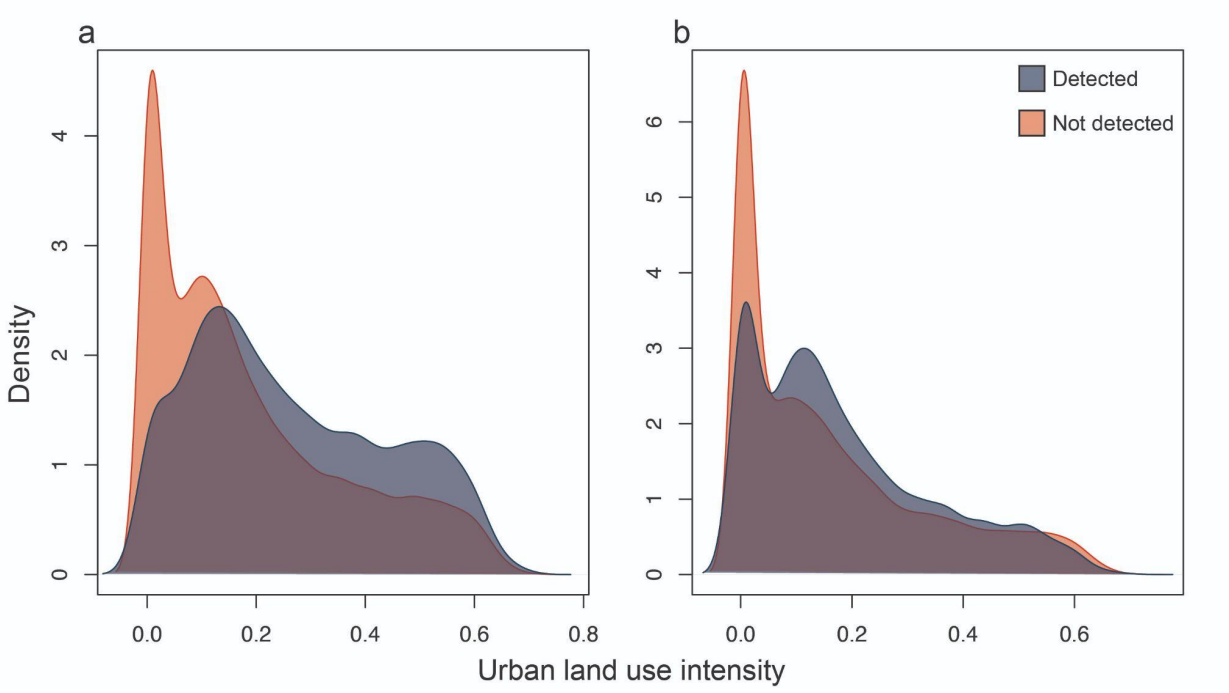

Figure 4. Kernel density plots showing the distribution of urban land use intensity values for (a) American black duck and (b) bobolink at locations where each species was detected (blue) and not detected (orange).

Interestingly, current flow was high on developed lands for both black ducks and bobolinks (Fig. 3b,c), suggesting substantial movement through suburban and urban landscapes. Despite our attempts to correct for eBird sampling bias through spatiotemporal subsampling (see above), high predicted movement through developed areas (and correspondingly high predicted habitat suitability, Fig. 2b,c) may stem in part from the tendency of community scientists to collect data in or near the cities in which they live. However, comparing detection/non-detection data for black ducks and bobolinks suggests that encounter rates for these species are indeed higher in more developed areas; the distribution of urban land use intensities (L) at locations where birds were detected was shifted towards higher urban L values relative to non-detection locations (Fig. 4) despite both detection and non-detection checklists having the same potential for spatial bias towards urban areas. For black ducks, the fact that many urban areas are situated along coastal or

inland waterways may explain this apparent preference for urbanized landscapes as stopover habitat. The drivers of the apparent bobolink preference for moderate levels of urban *L* are less obvious, but may reflect use of open grassy habitats in suburban lawns and urban greenspaces.

All three focal species considered here have experienced substantial declines or range contractions over the last several decades, with agricultural expansion and intensification implicated as a major driver in each case (Shirk et al. 2017, English et al. 2017, Stanton et al. 2018). However, our results suggest that, when managed wildlife-friendly practices (i.e., low-intensity grazing, moderate mowing or harvest frequency), agricultural landscapes can provide valuable movement habitat for sage grouse and bobolinks, while black ducks may benefit from access to agricultural lands in the non-migratory seasons, particularly when these are in proximity to native vegetation and/or wetland habitats. As noted above, federal incentive programs have an important role to play in supporting agricultural management practices that facilitate connectivity for these species, and we anticipate that our model results will be valuable in identifying target landscapes for such incentives.

References

BirdLife International and Handbook of the Birds of the World (2016a). *Centrocercus urophasianus*. The IUCN Red List of Threatened Species. Version 2021-3. https://www.iucnredlist.org. Downloaded on 09 December 2021.

BirdLife International and Handbook of the Birds of the World (2016b). *Dolichonyx oryzivorus*. The IUCN Red List of Threatened Species. Version 2021-3. https://www.iucnredlist.org. Downloaded on 06 January 2022.

BirdLife International and Handbook of the Birds of the World (2021). *Anas rubripes*. The IUCN Red List of Threatened Species. Version 2021-3. https://www.iucnredlist.org. Downloaded on 06 January 2022.

Bollinger, E. K., and T. A. Gavin. 2004. Responses of Nesting Bobolinks (Dolichonyx Oryzivorus) to Habitat Edges. The Auk 121:767–776.

Buttrick, S., K. Popper, M. Schindel, B. H. McRae, B. Unnasch, A. Jones, and J. Platt. 2015. Conserving Nature's Stage: Identifying Resilient Terrestrial Landscapes in the Pacific Northwest. The Nature Conservancy, Portland, Oregon.

Cava, J. A., N. G. Perlut, and S. E. Travis. 2016. Why come back home? Investigating the proximate

factors that influence natal philopatry in migratory passerines. Animal Behaviour 118:39–46.

Coluccy, J. M., K. A. Anderson, T. Yerkes, and J. L. Bowman. 2020. Migration routes and chronology of American Black Duck Anas rubripes. Wildfowl 70:148–166.

Connelly, J. W., M. A. Schroeder, A. R. Sands, and C. E. Braun. 2000. Guidelines to Manage Sage Grouse Populations and Their Habitats. Wildlife Society Bulletin (1973-2006) 28:967–985.

Conroy, M. J., M. W. Miller, and J. E. Hines. 2002. Identification and Synthetic Modeling of Factors Affecting American Black Duck Populations. Wildlife Monographs:1–64.

Courter, J. R., R. J. Johnson, C. M. Stuyck, B. A. Lang, and E. W. Kaiser. 2013. Weekend bias in Citizen Science data reporting: implications for phenology studies. International Journal of Biometeorology 57:715–720.

Cross, T. B., D. E. Naugle, J. C. Carlson, and M. K. Schwartz. 2017. Genetic recapture identifies long-distance breeding dispersal in Greater Sage-Grouse (Centrocercus urophasianus). The Condor 119:155–166.

CSP. 2019. Methods and approach used to estimate the loss and fragmentation of natural lands in the conterminous U.S. from 2001 to 2017. Technical Report, Truckee, CA.

CSP. 2020. Description of the approach, data, and analytical methods used for the Farms Under Threat: State of the States project, version 2.0. Final Technical Report. Truckee, CA.

Cutler, D. R., T. C. Edwards Jr., K. H. Beard, A. Cutler, K. T. Hess, J. Gibson, and J. J. Lawler. 2007. Random Forests for Classification in Ecology. Ecology 88:2783–2792.

Dewitz, J. 2019. National Land Cover Database (NLCD) 2016 Products: U.S. Geological Survey data release.

Dickson, B. G., C. M. Albano, R. Anantharaman, P. Beier, J. Fargione, T. A. Graves, M. E. Gray, K. R. Hall, J. J. Lawler, P. B. Leonard, C. E. Littlefield, M. L. McClure, J. Novembre, C. A. Schloss, N. H. Schumaker, V. B. Shah, and D. M. Theobald. 2019. Circuit-theory applications to connectivity science and conservation. Conservation Biology 33:239–249.

Doherty, K. E., D. E. Naugle, B. L. Walker, and J. M. Graham. 2008. Greater Sage-Grouse Winter Habitat Selection and Energy Development. The Journal of Wildlife Management 72:187–195.

Doherty, T. S., and D. A. Driscoll. 2018. Coupling movement and landscape ecology for animal conservation in production landscapes. Proceedings of the Royal Society B: Biological Sciences 285:20172272.

Dunn, P. O., and C. E. Braun. 1986. Late Summer-Spring Movements of Juvenile Sage Grouse. The Wilson Bulletin 98:83–92.

English, M. D., G. J. Robertson, L. E. Peck, and M. L. Mallory. 2017. Agricultural food resources and the foraging ecologies of American black ducks (Anas rubripes) and mallards (Anas platyrhynchos)

at the northern limits of their winter ranges. Urban Ecosystems 20:1311–1318.

Fahrig, L., J. Baudry, L. Brotons, F. G. Burel, T. O. Crist, R. J. Fuller, C. Sirami, G. M. Siriwardena, and J.-L. Martin. 2011. Functional landscape heterogeneity and animal biodiversity in agricultural landscapes. Ecology Letters 14:101–112.

Fajardo, N., A. M. Strong, N. G. Perlut, and N. J. Buckley. 2009. Natal and Breeding Dispersal of Bobolinks (Dolichonyx oryzivorus) and Savannah Sparrows (Passerculus sandwichensis) in an Agricultural Landscape. The Auk 126:310–318.

Fehlmann, G., M. J. O'riain, I. FÜrtbauer, and A. J. King. 2021. Behavioral Causes, Ecological Consequences, and Management Challenges Associated with Wildlife Foraging in Human-Modified Landscapes. BioScience 71:40–54.

Fleiss, J. L., B. Levin, and M. C. Paik. 2013. Statistical Methods for Rates and Proportions. John Wiley & Sons.

Fox, E. W., R. A. Hill, S. G. Leibowitz, A. R. Olsen, D. J. Thornbrugh, and M. H. Weber. 2017. Assessing the accuracy and stability of variable selection methods for random forest modeling in ecology. Environmental Monitoring and Assessment 189:316.

Franke, J., V. Keuck, and F. Siegert. 2012. Assessment of grassland use intensity by remote sensing to support conservation schemes. Journal for Nature Conservation 20:125–134.

Gómez Giménez, M., R. de Jong, R. Della Peruta, A. Keller, and M. E. Schaepman. 2017. Determination of grassland use intensity based on multi-temporal remote sensing data and ecological indicators. Remote Sensing of Environment 198:126–139.

Gorelick, N., M. Hancher, M. Dixon, S. Ilyushchenko, D. Thau, and R. Moore. 2017. Google Earth Engine: Planetary-scale geospatial analysis for everyone. Remote Sensing of Environment 202:18–27.

Grass, I., J. Loos, S. Baensch, P. Batáry, F. Librán-Embid, A. Ficiciyan, F. Klaus, M. Riechers, J. Rosa, J. Tiede, K. Udy, C. Westphal, A. Wurz, and T. Tscharntke. 2019. Land-sharing/-sparing connectivity landscapes for ecosystem services and biodiversity conservation. People and Nature 1:262–272.

Hastie, T., R. Tibshirani, and J. Friedman. 2009. The Elements of Statistical Learning: Data Mining, Inference, and Prediction. Second edition. Springer, New York, NY.

Hendershot, J. N., J. R. Smith, C. B. Anderson, A. D. Letten, L. O. Frishkoff, J. R. Zook, T. Fukami, and G. C. Daily. 2020. Intensive farming drives long-term shifts in avian community composition. Nature 579:393–396.

Herkert, J. R. 1997. Bobolink Dolichonyx oryzivorus population decline in agricultural landscapes in the Midwestern USA. Biological Conservation 80:107–112.

Homer, C. G., T. C. Edwards, R. D. Ramsey, and K. P. Price. 1993. Use of Remote Sensing Methods in Modelling Sage Grouse Winter Habitat. The Journal of Wildlife Management 57:78–84.

Johnston, A., W. M. Hochachka, M. E. Strimas-Mackey, V. R. Gutierrez, O. J. Robinson, E. T. Miller, T. Auer, S. T. Kelling, and D. Fink. 2021. Analytical guidelines to increase the value of community science data: An example using eBird data to estimate species distributions. Diversity and Distributions 27:1265–1277.

Keeley, A. T. H., P. Beier, and J. W. Gagnon. 2016. Estimating landscape resistance from habitat suitability: effects of data source and nonlinearities. Landscape Ecology 31:2151–2162.

Kremen, C., and A. M. Merenlender. 2018. Landscapes that work for biodiversity and people. Science 362.

Landau, V. A., V. B. Shah, R. Anantharaman, and K. R. Hall. 2021. Omniscape.jl: Software to compute omnidirectional landscape connectivity. Journal of Open Source Software 6:2829.

LANDFIRE. 2016. Existing Vegetation Type Layer, LANDFIRE 2.0.0. U.S. Department of the Interior, Geological Survey, and U.S. Department of Agriculture.

Lieske, D. J., B. Pollard, M. Gloutney, R. Milton, K. Connor, R. Dibblee, G. Parsons, and D. Howerter. 2012. The Importance of Agricultural Landscapes as Key Nesting Habitats for the American Black Duck in Maritime Canada. Waterbirds 35:525–534.

Luck, G. W., T. H. Ricketts, G. C. Daily, and M. Imhoff. 2004. Alleviating spatial conflict between people and biodiversity. Proceedings of the National Academy of Sciences 101:182–186.

Maisonneuve, C., L. Bélanger, D. Bordage, B. Jobin, M. Grenier, J. Beaulieu, S. Gabor, and B. Filion. 2006. American Black Duck and Mallard Breeding Distribution and Habitat Relationships along a Forest-Agriculture Gradient in Southern Québec. The Journal of Wildlife Management 70:450–459.

Malley, J. D., J. Kruppa, A. Dasgupta, K. G. Malley, and A. Ziegler. 2012. Probability Machines: Consistent probability estimation using nonparametric learning machines. Methods of Information in Medicine 51:74–81.

McRae, B. H., B. G. Dickson, T. H. Keitt, and V. B. Shah. 2008. Using circuit theory to model connectivity in ecology, evolution, and conservation. Ecology 89:2712–2724.

McRae, B., K. Popper, A. Jones, M. Schindel, S. Buttrick, K. Hall, R. Unnasch, and J. Platt. 2016. Conserving nature's stage: Mapping omnidirectional connectivity for resilient terrestrial landscapes in the Pacific Northwest. The Nature Conservancy, Portland, OR.

Morton, J. M., R. L. Kirkpatrick, M. R. Vaughan, and F. Stauffer. 1989. Habitat Use and Movements of American Black Ducks in Winter. The Journal of Wildlife Management 53:390–400.

Murray, N. J., S. R. Phinn, M. DeWitt, R. Ferrari, R. Johnston, M. B. Lyons, N. Clinton, D. Thau, and R.

A. Fuller. 2019. The global distribution and trajectory of tidal flats. Nature 565:222–225.

Newbold, T., L. N. Hudson, S. L. L. Hill, S. Contu, I. Lysenko, R. A. Senior, L. Börger, D. J. Bennett, A. Choimes, B. Collen, J. Day, A. De Palma, S. Díaz, S. Echeverria-Londoño, M. J. Edgar, A. Feldman, M. Garon, M. L. K. Harrison, T. Alhusseini, D. J. Ingram, Y. Itescu, J. Kattge, V. Kemp, L. Kirkpatrick, M. Kleyer, D. L. P. Correia, C. D. Martin, S. Meiri, M. Novosolov, Y. Pan, H. R. P. Phillips, D. W. Purves, A. Robinson, J. Simpson, S. L. Tuck, E. Weiher, H. J. White, R. M. Ewers, G. M. Mace, J. P. W. Scharlemann, and A. Purvis. 2015. Global effects of land use on local terrestrial biodiversity. Nature 520:45–50.

Oyler-Mccance, S. J., S. E. Taylor, and T. W. Quinn. 2005. A multilocus population genetic survey of the greater sage-grouse across their range. Molecular Ecology 14:1293–1310.

Peck, L. E., M. D. English, G. J. Robertson, S. R. Craik, and M. L. Mallory. 2022. Migration chronology and movements of adult American black ducks Anas rubripes wintering in Nova Scotia, Canada. Wildlife Biology 2022.

Perlut, N. G. 2018. Prevalent transoceanic fall migration by a 30-gram songbird, the Bobolink. The Auk 135:992–997.

Perlut, N. G., A. M. Strong, T. M. Donovan, and N. J. Buckley. 2008. Regional population viability of grassland songbirds: Effects of agricultural management. Biological Conservation 141:3139–3151.

R Core Team. 2021. R: A language and environment for statistical computing. R Foundation for Statistical Computing, Vienna, Austria.

Redlich, S., E. A. Martin, B. Wende, and I. Steffan-Dewenter. 2018. Landscape heterogeneity rather than crop diversity mediates bird diversity in agricultural landscapes. PLOS ONE 13:e0200438.

Robinson, O. J., C. P. McGowan, and P. K. Devers. 2016. Updating movement estimates for American black ducks (Anas rubripes). PeerJ 4:e1787.

Robinson, O. J., V. Ruiz-Gutierrez, and D. Fink. 2018. Correcting for bias in distribution modelling for rare species using citizen science data. Diversity and Distributions 24:460–472.

Sacks, W. J., D. Deryng, J. A. Foley, and N. Ramankutty. 2010. Crop planting dates: an analysis of global patterns. Global Ecology and Biogeography 19:607–620.

Sappington, J. M., K. M. Longshore, and D. B. Thompson. 2007. Quantifying Landscape Ruggedness for Animal Habitat Analysis: A Case Study Using Bighorn Sheep in the Mojave Desert. The Journal of Wildlife Management 71:1419–1426.

Shirk, A. J., M. A. Schroeder, L. A. Robb, and S. A. Cushman. 2017. Persistence of greater sage-grouse in agricultural landscapes. The Journal of Wildlife Management 81:905–918.

Sieving, K. E., M. F. Willson, and T. L. De Santo. 1996. Habitat Barriers to Movement of Understory

Birds in Fragmented South-Temperate Rainforest. The Auk 113:944–949.

Stanton, R. L., C. A. Morrissey, and R. G. Clark. 2018. Analysis of trends and agricultural drivers of farmland bird declines in North America: A review. Agriculture, Ecosystems & Environment 254:244–254.

Stevens, C. E., T. S. Gabor, and A. W. Diamond. 2003. Use of Restored Small Wetlands by Breeding Waterfowl in Prince Edward Island, Canada. Restoration Ecology 11:3–12.

Strimas-Mackey, M., W. M. Hochachka, V. Ruiz-Gutierrez, O. J. Robinson, E. T. Miller, T. Auer, S. Kelling, D. Fink, and A. Johnston. 2020. Best Practices for Using eBird Data. Version 1.0. Cornell Lab of Ornithology, Ithaca, New York.

Strimas-Mackey, M., E. Miller, and W. Hochachka. 2018. auk: eBird Data Extraction and Processing with AWK. R package version 0.3. 0.

Sullivan, B. L., J. L. Aycrigg, J. H. Barry, R. E. Bonney, N. Bruns, C. B. Cooper, T. Damoulas, A. A. Dhondt, T. Dietterich, A. Farnsworth, D. Fink, J. W. Fitzpatrick, T. Fredericks, J. Gerbracht, C. Gomes, W. M. Hochachka, M. J. Iliff, C. Lagoze, F. A. La Sorte, M. Merrifield, W. Morris, T. B. Phillips, M. Reynolds, A. D. Rodewald, K. V. Rosenberg, N. M. Trautmann, A. Wiggins, D. W. Winkler, W.-K. Wong, C. L. Wood, J. Yu, and S. Kelling. 2014. The eBird enterprise: An integrated approach to development and application of citizen science. Biological Conservation 169:31–40.

Tack, J. D., A. F. Jakes, P. F. Jones, J. T. Smith, R. E. Newton, B. H. Martin, M. Hebblewhite, and D. E. Naugle. 2019. Beyond protected areas: Private lands and public policy anchor intact pathways for multi-species wildlife migration. Biological Conservation 234:18–27.

Tack, J. D., D. E. Naugle, J. C. Carlson, and P. J. Fargey. 2012. Greater sage-grouse Centrocercus urophasianus migration links the USA and Canada: a biological basis for international prairie conservation. Oryx 46:64–68.

Takaku, J., T. Tadono, K. Tsutsui, and M. Ichikawa. 2016. Validation of "AW3D" global DSM generated from ALOS PRISM. ISPRS Annals of Photogrammetry, Remote Sensing & Spatial Information Sciences 3.

Theobald, D. M. 2013. A general model to quantify ecological integrity for landscape assessments and US application. Landscape Ecology 28:1859–1874.

Thornton, M. M., R. Shrestha, Y. Wei, P. E. Thornton, S.-C. Kao, and B. E. Wilson. 2020. Daymet: Daily Surface Weather Data on a 1-km Grid for North America, Version 4. ORNL DAAC.

USDA. 2012. Plant Hardiness Zone Map. https://planthardiness.ars.usda.gov/.

USGS. 2020. U.S Geological Survey (USGS) Gap Analysis Project (GAP). Protected Areas Database of the United States (PAD-US) 2.1: U.S. Geological Survey data release.

Wimberly, M. C., D. M. Narem, P. J. Bauman, B. T. Carlson, and M. A. Ahlering. 2018. Grassland connectivity in fragmented agricultural landscapes of the north-central United States. Biological Conservation 217:121–130.

Wright, M. N., and A. Ziegler. 2017. ranger: A Fast Implementation of Random Forests for High Dimensional Data in C++ and R. Journal of Statistical Software 77:1–17.

Zeller, K. A., S. A. Cushman, N. J. Van Lanen, J. D. Boone, and E. Ammon. 2021. Targeting conifer removal to create an even playing field for birds in the Great Basin. Biological Conservation 257:109130.

Zeller, K. A., K. McGarigal, and A. R. Whiteley. 2012. Estimating landscape resistance to movement: a review. Landscape Ecology 27:777–797.

Appendix A. Estimating human land use intensity

To evaluate the influence that agricultural lands and other modified landscapes exert on avian connectivity, we estimated human land use intensity (*L*) for all locations (i.e., pixels in a gridded landscape) across CONUS. Our estimates of human land use intensity were based on a procedure originally described by Theobald (2013), which assigns literature-supported values of intensity to multiple forms of human land use. For all non-agricultural land uses we used an existing *L* model (CSP 2019) that integrates multiple land use variables into three human impact categories - urban (including data on residential development and nighttime lights), transportation (including roads, railways, powerlines, and pipelines), and energy (including oil and gas wells, coal mines, and utility-scale solar and wind installations).

To quantify land use intensity on agricultural lands, we started with existing, static *L* estimates for individual agricultural cover types (Theobald 2013) and incorporated a dynamic measure of management intensity based on temporal variation in vegetation cover at a given location. We used high spatial resolution (10 m) data on 2016 land cover from American Farmland Trust's Farms Under Threat (FUT) analysis, which integrates data from multiple national-scale datasets to define several agricultural and non-agricultural cover classes (CSP 2020; data accessible from csp-fut.appspot.com). We focused on the four agricultural cover classes, which together account for 3.64 million km^2, or approximately 47.6% of CONUS land area (Fig. 1). These agricultural classes are cropland (1,549,077 km^2 across CONUS), pasture (430,369 km^2), rangeland (1,658,472 km^2), and woodland (174,323 km^2). The woodland class is a subset of the Natural Resources Inventory forest class defined as "natural or planted forested cover that is part of a functioning farm unit" and is no more than 160 m from cropland or pasture (CSP 2020). We assigned each of these four classes with a baseline value of land-use intensity (*L*) corresponding with the general level of human disturbance associated with that agricultural type. For cropland and pasture, baseline *L* values of 0.5 and 0.4, respectively, were taken from Theobald (2013). Similar approaches to modeling ecological flow and/or landscape integrity have treated rangelands as having lower impact than cropland or pasture because rangelands tend to retain some natural vegetation cover and have relatively limited human influence (Buttrick et al. 2015, McRae et al. 2016). Woodlands are similarly characterized by relatively natural vegetation cover, albeit in close proximity to managed agricultural lands. We therefore assigned a baseline *L* value

of 0.2 to both rangelands and woodlands in an effort to capture the greater potential for wildlife movement through these cover types.

For both cropland and pasture, the agricultural cover types characterized by relatively intensive human management, we allowed *L* values to vary between pixels of the same cover type based on estimates of management intensity. Management intensity estimates were derived from temporal variability in vegetation cover based on the assumption that more intensively managed areas (e.g., croplands with high fertilizer inputs and/or multiple harvests per year; pasture subject to a high mowing frequency) will have greater variability in vegetation cover during the growing season than areas subject to less human intervention (e.g., fallow fields) (Franke et al. 2012, Gómez Giménez et al. 2017). We used a timeseries of Normalized Difference Vegetation Index (NDVI) values to estimate vegetation cover variability, acquiring cloud-free NDVI estimates at 16-day intervals from NASA's MODIS system (MOD13Q1 products). For each cropland and pasture pixel across CONUS, we used NDVI estimates over a five year period (2014-2018) centered on 2016, the year of our land cover dataset. NDVI estimates were acquired during the growing season for each year, with growing season start and end dates defined separately for each U.S. state based on the planting dates database developed by Sacks et al. (2010). For each U.S. state, we extracted the planting start date and harvest end date for a common crop type and used this as the date range within which NDVI estimates were acquired for all cropland and pasture pixels in that state. For consistency, we used corn as the crop type to define growing season dates for all states where corn is grown. For states where corn is not grown, we used another spring-planted crop represented in the database (spring barley in Nevada and potatoes in Maine, Massachusetts, and Rhode Island). For states that are absent from the database (Connecticut, Vermont, and New Hampshire), we used the planting start and harvest end dates for nearby states (in this case, other states in the New England region).

For each pixel of cropland and pasture, we calculated the coefficient of variation for all NDVI values across the time series (hereafter, cvNDVI) as our estimate of vegetation cover variability. The coefficient of variation was chosen to account for differences between vegetation types (e.g., different crops) and geographic location in average plant greenness. For each cover type (cropland or pasture), we centered cvNDVI values by first calculating the mean for all pixels of

that cover type within the same USDA plant hardiness zone (PHZ; (USDA 2012)) and then subtracting this mean value from the value for each pixel. PHZs describe bands of average annual minimum winter temperature across CONUS. We centered cvNDVI values based on means within a PHZ to account for potential differences in vegetation cover variability across latitudes and climatic conditions (e.g., lower variability in areas with shorter growing seasons). Averages (± SD) of mean-centered cvNDVI were -0.05 (± 0.13) and -0.03 (± 0.10) for cropland and pasture, respectively. To derive the final *L* value for cropland and pasture pixels, mean-centered cvNDVI values were added to the baseline *L* value for each cover type (0.5 for cropland and 0.4 for pastureland, see above), resulting in a range of final *L* estimates centered on the baseline value. Thus, pixels with lower than average vegetation cover variability for a given cover type and PHZ (i.e., negative mean-centered cvNDVI) received *L* values below the baseline value for that cover type and those with higher than average variability (positive mean-centered cvNDVI) received *L* values above the baseline. For rangeland and woodland, we did not incorporate vegetation index data into *L* estimates, instead using baseline *L* values for all pixels under the assumption that variability in NDVI will be more strongly associated with phenology and plant community composition than with human management intensity in the cover types characterized by relatively natural vegetation.